Automated RF Tomographic Imaging of Utility Poles Above and Below Ground

Dr David G Johnson & Dr Graham M Brooker
Australian Centre for Field Robotics
The University of Sydney
Sydney, NSW 2006, Australia
d.johnson@acfr.usyd.edu.au

***Abstract*— This paper describes the development of a 3-D scanning system and associated signal processing for carrying out non-destructive imaging of wooden utility poles. While nominally rod-shaped, natural variations in the original tree, its cut, and any attached street furniture impose considerable complexity to automating the task of scanning a pole. While RF tomographic techniques are theoretically capable of producing images of sufficient quality to assess pole degradation, spectrum constraints; the need for a low-cost, efficient and reliable scanning device and the additional complexity of making sub-surface measurements through heterogeneous material combine to make this a challenging task. Ground-truth data obtained from a medical CAT scanner and a customised experimental apparatus are described, along with progress made in the selection of appropriate scanning and processing mechanisms.**

Keywords— RF Tomography; Ultra-Wideband (UWB) radar; Ground-penetrating radar (GPR)

I. Introduction

There are over 1 million wooden power poles in the Australian state of Victoria alone, which with a lifespan of approximately 50 years must be manually assessed for structural integrity at least once every 10 years; more often once initial decay is identified. Such an assessment is typically carried out by trained operators, taking drilled core-samples at accessible points on the 'trunk' of the pole, i.e. 0 to 2m above ground and, if mandated, excavating up to 0.5m below-ground. This assessment is obviously a major undertaking and therefore multiple attempts have been made to assess more-efficient and more accurate non-destructive means of determining pole integrity over the years. Such methods as X-ray, acoustic and radar have each been assessed [1] and a number of commercial products exist that provide a hand-held tool for operators, yet none-to-date have made a significant impact compared to the more traditional invasive methods.

Having expertise and equipment spanning much of the microwave and millimetre-wave spectra, the *Australian Centre for Field Robotics* (ACFR) was initially approached to compare microwave and THz imaging methods [2] that could potentially utilise the sophistication of modern robotic sensor-fusion techniques to provide a fast automated scanning system. It was rapidly determined using our W-band (90-100GHz) radar test-bed [3], that the rapidly fluctuating radar cross section due to surface imperfections would be extremely difficult to overcome without a precise geometric surface model, leaving little additional information relating to sub-surface defects to be inferred. Further penetration tests were undertaken by placing a rotating 100m^2 trihedral corner reflector (at 94GHz) behind increasing thicknesses of wood. These confirmed the poor penetration capability of the *millimeter-wave* (MMW) radar signal, as with wood thicknesses above 3cm the target became undetectable, indicating attenuation of > 70dB.

Results in the microwave region (1-8GHz) were more encouraging, with data collected in both bi-static (transmission-mode) and quasi-monostatic (reflection-mode) configurations promising high-quality *radio-frequency* (RF) tomographic image capability for above-ground measurements. The subsequent need for below-ground imaging was then examined as an extension to the system.

The remainder of this paper will therefore be set out as follows: Section II describes the experimental setup constructed for performing above and below ground tomographic measurements, Section III describes the formation of ground-truth measurements made by placing our 1m-length serviceable, 'good', and out-of-service, 'bad', utility-pole samples within a medical *computerized axial tomography* (CAT) scanner, Section IV describes the RF tomographic results so far produced by our system, while Section V provides Conclusions and Future Work.

II. Experimental Setup

A. Above Ground Measurements

It is anticipated that an 'in-field' system will likely incorporate a scanning mechanism mounted on a robotic arm with multiple degrees of freedom, allowing access from a range of perspectives and potentially access to the cross-arm commonly located at the top of the pole. For the initial tests however, a less complex system based on rotating a section of pole within the confines of a static antenna rig was built, as seen in Figure 1. The two QPar Angus 2-18GHz broadband horn antennas were then connected to a Keysight N9917A (FieldFox) *vector network analyser* (VNA) operating between 0 and 18 GHz with an output power of +3dBm.

This work is supported by the Australian Centre for Field Robotics and Select Solutions, a division of AusNet Services Pty Ltd.

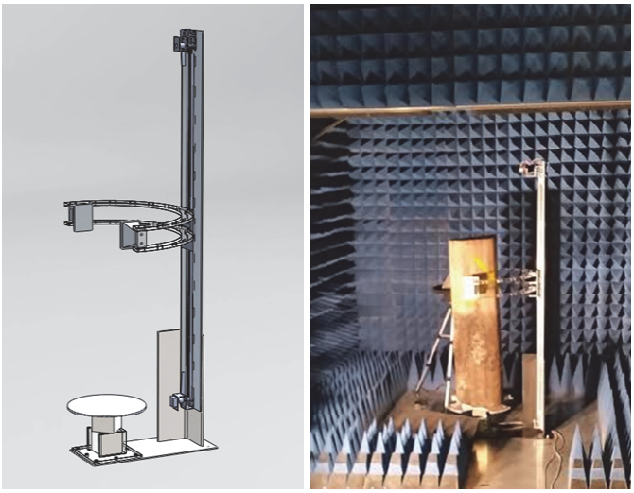

Fig. 1. Schematic of transmission-mode pole-scanning mechanism and a sample pole mounted within ACFR's anechoic chamber.

The system shown in Fig. 1 provided obvious benefits as well as one or two unforeseen consequences:

Pros:

- It provided a controlled environment in which measurements could be made repeatedly and accurately with an angular precision of 0.01° and vertical precision of 1mm.
- It allowed poles of varying diameter (up to 45cm or ~150kg) to be scanned in varying quasi-monostatic or bistatic configurations.
- The linear antenna rail could be easily removed, either to allow far-field MMW measurements or installation of the below-ground test apparatus.

Cons:

- The difficulty in vertically mounting a rotten 100kg wooden pole to a small but powerful actuated motor (Schunk PowerCube PR090) was not apparent until attempted, both in its installation within the chamber and in achieving alignment of the axis of revolution with the (fairly arbitrary) central axis of the trunk.
- Considerable effort was placed on ensuring a rigid scanning mechanism, with the drawback that this limited the vertical extent of the pole that could then be scanned.
- Storage of the good and bad pole samples in an indoor environment over an extended period of time appears to have led to some additional drying and cracking of both samples, such that the 'good' pole may now be considered merely 'less-bad'.

B. *Below-Ground Measurements*

In order to maintain the positive aspects of the above-ground measurements already described, an 'earth-proxy' arrangement was constructed allowing continual rotation of the pole sample as seen in Fig. 2 (with the linear antenna translation rail removed). The annulus was elevated to ensure that the imaged region coincided with that of the above-ground measurements. As most utility poles are buried

Fig. 2. Before and after shots of a 300mm deep by 1m diameter annulus filled with soil and sand, surrounding a rotating pole sample. 6dBi (ground-penetrating) wideband whip antennas are shown in transmission-mode.

predominantly in sand, which incidentally has a similar dielectric constant to dry wood of ~2-6 [4], the earth was made up of alternate quadrants of sand and potting mix. By placing a valve in the base of the annulus, moisture levels may also be varied, albeit in an ad-hoc manner. Based on similar concepts from borehole-radar systems in the mining industry and tunnel-detection systems investigated by the US military [5-6], a simple penetration scheme based on directly inserting plastic coated whip antennas into the earth was attempted (with moderate success) in both transmission-mode and reflection-mode as before. An obvious issue that can be seen from Fig. 2 is the protrusion of the whip antennas from the soil that is likely to significantly alter the manner in which energy is transferred to the pole. An alternate antenna system based on more compact and directive UWB patch antennas on FR4 substrate is currently underway [7].

III. CAT Scanned Ground Truth

Based on an existing relationship with the University of Sydney's Faculty of Health Sciences we were able to perform CAT-scan imaging of both the good and bad pole samples in order to build up a full 3-D ground truth representation of the internal structure of each pole, example slices of which are seen in Fig. 3(a) & (b) respectively. Based on the performance

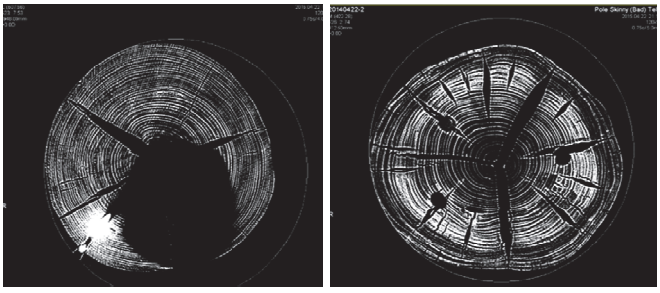

(a) (b)

Fig. 3. CAT slices of (a) 'good' and (b) 'bad' pole samples.

of the CAT scan machine, commissioned in 2014 [8], these images provide possibly the most accurate representation of the internal structure of a tree-trunk ever made. Unfortunately, due to an initial problem with determining the correct parameters for scanning wooden poles using a machine designed for medical imaging, the good pole has a mask applied intended for imaging lungs.

Sufficient information remains however, to allow several observations to be made impacting on the corresponding RF tomography results:

- A 40cm circle has been super-imposed on each image showing the variation in size and irregular shape of each pole.
- While growth-rings and some cracks are visible in both samples, the more numerous and wider cracks of the bad pole close to the outer edge and variation in internal density, explain why it was slated for removal from service.
- Also visible in the good pole is the bright response from a large embedded nail, while in the bad pole cuts across three of the many drilled core-holes can be seen.

Not seen in our pole samples, but potentially common in a real-world environment are the road-signs and other metallic infrastructure typically mounted to roadside utility poles. These are likely to place additional challenges both on the kinematics of moving a robotic scanning system safely around such obstacles and in the spurious response on the images that will result, similar to the embedded nail.

IV. Experimental Results

A. Above-Ground Measurements

Initial measurements in the microwave regime were made between 10MHz and 18GHz, the full bandwidth of the FieldFox. It was quickly established, as seen in Fig. 4, that little radiation was able to penetrate above 7GHz, while the lower cut-off frequency of the broadband antennas gave little response below 1.5GHz. Combined with restrictions in spectral compliance according to Australian *Low Interference Potential Device* (LIPD) legislation [9], this led us to limit subsequent measurements to the 1-8GHz region.

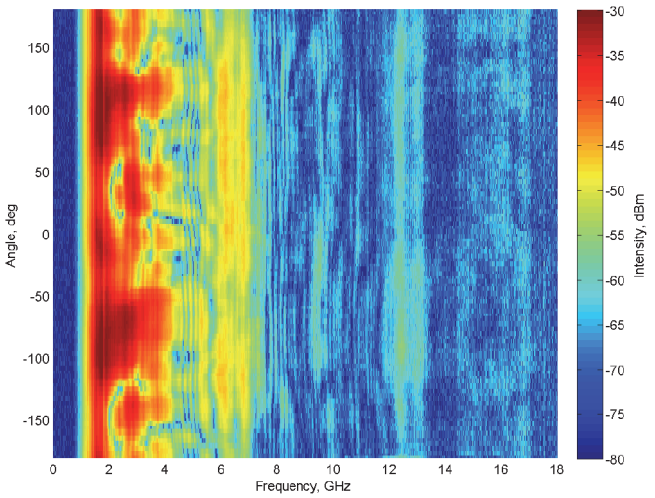

Fig. 4. Raw frequency vs. angle data for bad pole measured in transmission-mode configuration after mean-signal subtraction.

The bad pole results shown in Fig. 5 for raw-frequency, range-profile and tomographic data respectively indicate the quality of image possible from one of the simplest forms of tomographic reconstruction, namely filtered back-projection [10]. In comparison to Fig. 4 it can be seen that strong returns appear across the frequency band leading to a sharply defined primary return from the surface of the pole as opposed to the transmission response that must cross the entire pole and is therefore attenuated strongly at higher frequencies. Fig. 5(c) therefore shows a distinct air-pole interface response although some internal structure can easily be made out. An issue with the experimental setup highlighted earlier, i.e. the misalignment from vertical of the pole sample, is believed to have led to some de-focusing of the tomographic image. This will be a challenging but surmountable issue for the next-generation robotic scanning mechanism whose kinematics will be known with more certainty.

B. Below-Ground Measurements

Equivalent transmission-mode measurements to Fig. 4. (as described by the apparatus configuration shown in Fig. 2) were then used to determine that the below ground sensitivity of the 6dBi whip antennas dropped off below 3GHz. The set of measurements was therefore constrained between 100MHz and 3GHz, again with a power output of +3dBm, the upper limit of the FieldFox in S21 mode.

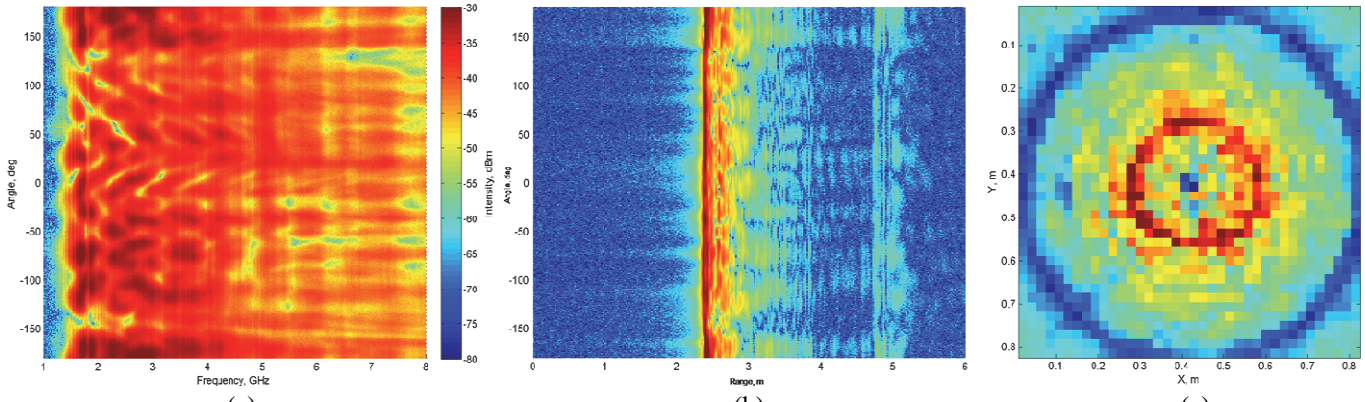

(a) (b) (c)

Fig. 5. (a) Above-ground raw-frequency vs. angle data for bad pole in reflection-mode configuration (after mean-signal subtraction). (b) Corresponding range-profile vs. angle data. (c) Corresponding RF tomographic slice after filtered-back-projection.

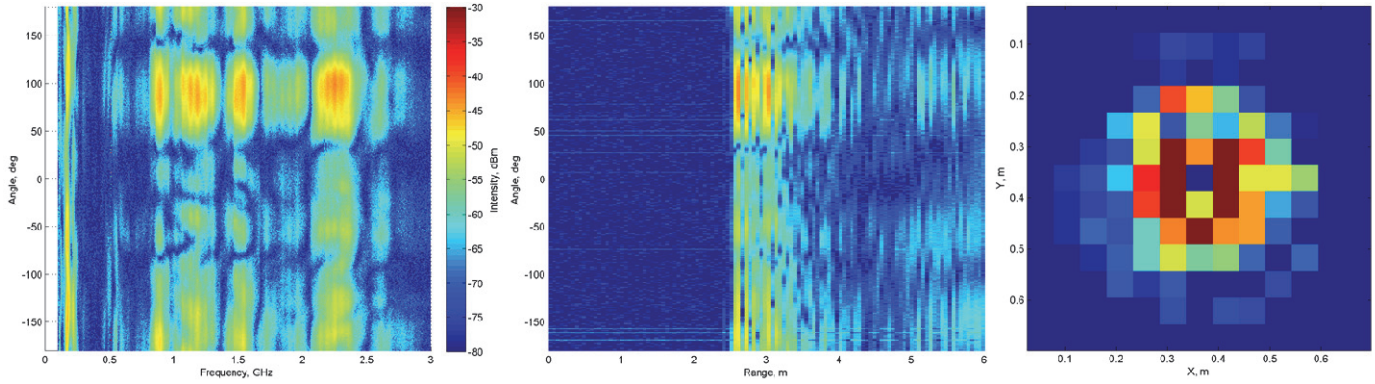

(a) (b) (c)

Fig. 6. (a) Below-ground raw-frequency vs. angle data for bad pole in reflection-mode configuration (after mean-signal subtraction). (b) Corresponding range-profile vs. angle data. (c) Corresponding RF tomographic slice after filtered-back-projection.

The corresponding reflection-mode results for the below-ground dataset are shown in Fig. 6. These data show considerably less variation with angle, decreased signal strength and the reduced bandwidth leads to an obvious worsening of resolution. However the fact that this simple setup has apparently identified the void at the centre of the pole, which is likely the only constant factor over the increased length of the pole within the elevation beam-width of the antennas at this low frequency, is encouraging.

It remains to be seen whether more directive antennas (entirely buried within the sand/earth medium), greater transmit power or more sophisticated reconstruction algorithms are able to better discern features within the buried pole. An additional factor that must be taken into consideration is the moisture content of the soil, which will obviously lead to a further reduction in signal penetration.

Not shown here, for either above or below-ground measurements, are the tomographic results for the transmission-mode measurements. For the below-ground data in particular, poor signal-to-noise ratio (even in these dry conditions) proved insufficient to yield a tomographic image of good quality. Other techniques such as *truncated singular value decomposition* (T-SVD) and *algebraic reconstruction techniques* (ART) are currently under investigation to determine if increased performance can be realized [6,11].

V. Conclusions and Future Work

This paper described initial experiments to perform above and below ground tomographic imaging of utility poles in an automated manner. With the aim of maximizing imaging resolution under a LIPD class-license, full penetrative bandwidth was assessed and imaging results were compared qualitatively with ground truth provided by a medical-grade CAT scanner. Early results show a clear variation in returns that corresponds with the CT images and further work is now underway to investigate the application of more directive antennas and sophisticated reconstruction techniques.

It is also expected that with greater knowledge of the geometry of the complex pole surface additional means of minimizing the effects of the air-pole interface may be achieved, while also providing a collision-avoidance capability to the eventual robotically-actuated system. An additional concern with operating in the real-world is the acquisition speed of the scanning apparatus. While pulsed UWB systems offer one means of generating wide-band data much faster than a swept-system, these systems have their own issues and hardware constraints. An alternative solution under investigation is the use of broad-spectrum transmission and high-speed continuous sampling, e.g. as provided by the new Keysight N7081A VNA, which may provide an order of magnitude reduction in sampling time vs. traditional methods.

Acknowledgment

The authors wish to thank the University of Sydney's Faculty of Health Science, Javier Martinez and Dai Bang Nguyen, for performing the CAT-scans of the pole samples.

References

[1] A. Sundaram, "Evaluation of Wood Pole Condition Assessment Tools – Final Report", Electric Power Research Institute.1010654, 2005.

[2] C. M. Armstrong, "The Truth about Terahertz," Spectrum, IEEE, vol. 49, pp. 36-41, 2012.

[3] D. Johnson, et al., "Development of a Dual-Mirror-Scan Elevation-Monopulse Antenna System," in Radar Conference (EuRAD), 2011 European, pp. 281-284, 2011.

[4] S. Hubbard, et al., "Estimation of Permeable Pathways and Water Content using Tomographic Radar Data", The Leading Edge, 16, 1623-1628, 1997.

[5] C. Kemp, et al., "Imaging an Orebody Ahead of Mining Using Borehole Radar at the Snap Lake Diamond Mine, Northwest Territories, Canada", Seventh International Mining Geology Conference, Perth, WA. 2009.

[6] L. Lo Monte, et al., "Radio Frequency Tomography for Tunnel Detection," Geoscience and Remote Sensing, IEEE Transactions on, vol.48, no.3, pp.1128,1137, 2010.

[7] J. A. Gomez Escobar, "Through-Wall Radar Imaging using Non-Linear Ultra-Wideband Diffraction Tomography," PhD, The University of Sydney, 2011.

[8] L. Milkins, C. Moore and J. Spiteri, Simulation Based Education - Professional Entry Student Education and Training, Health Education Training Institute (HETI), 2014.

[9] IFC 60/2014: Proposal to Remake the LIPD Class Licence with Variations, Australian Communications and Media Authority, December 2014.

[10] F. Natterer and F. Wübbeling, "Mathematical Methods in Image Reconstruction". Philadelphia: Society for Industrial and Applied Mathematics, 2001.

[11] V Picco, et al., RF Tomography in Free Space: Experimental Validation of the Forward Model and an Inversion Algorithm Based on the Algebraic Reconstruction Technique, International Journal of Antennas and Propagation 06/2013; 2013.